Lipidomic Analysis of Microfat and Nanofat Reveals Different Lipid Mediator Compositions

Lisanne Grünherz, MD
Sedef Kollarik, PhD
Nadia Sanchez-Macedo, PhD
Michelle McLuckie, PhD
Nicole Lindenblatt, MD

Zurich, Switzerland

Background: Microfat and nanofat are commonly used in various surgical procedures, from skin rejuvenation to scar correction, to contribute to tissue regeneration. Microfat contains mainly adipocytes and is well suited for tissue augmentation, and nanofat is rich in lipids, adipose-derived stem cells, microvascular fragments, and growth factors, making it attractive for aesthetic use. The authors have previously demonstrated that the mechanical processing of microfat into nanofat significantly changes its proteomic profile. Considering that mechanical fractionation leads to adipocyte disruption and lipid release, they aimed to analyze their lipidomic profiles for their regenerative properties.
Methods: Microfat and nanofat samples were isolated from 14 healthy patients. Lipidomic profiling was performed by liquid chromatography tandem mass spectrometry. The resulting data were compared against the Human Metabolome and LIPID MAPS Structure Database. MetaboAnalyst was used to analyze metabolic pathways and lipids of interest.
Results: From 2388 mass-to-charge ratio features, metabolic pathway enrichment analysis of microfat and nanofat samples revealed 109 pathways that were significantly enriched. Microfat samples revealed higher-intensity levels of sphingosines, different eicosanoids, and fat-soluble vitamins. Increased levels of coumaric acids and prostacyclin were found in nanofat.
Conclusions: This is the first study to analyze the lipidomic profiles of microfat and nanofat, providing evidence that mechanical emulsification of microfat into nanofat leads to changes in their lipid profiles. From 109 biological pathways, antiinflammatory, antifibrotic, and antimelanogenic lipid mediators were particularly enriched in nanofat samples when compared with microfat. Although further studies are necessary for a deeper understanding of the composition of these specific lipid mediators in nanofat samples, the authors propose that they might contribute to its regenerative effects on tissue. *(Plast. Reconstr. Surg.* 154: 895e, 2024.)
Clinical Relevance Statement: Profiling the unique lipid mediators in nanofat and microfat enhances our understanding of their different therapeutic effects and allows us to link these specific mediators to antiinflammatory, proregenerative, or healing properties. Ultimately, this insight can advance personalized therapeutic strategies, where a specific type of fat is selected based on its optimal therapeutic effect.

From the Department of Plastic Surgery and Hand Surgery, University Hospital Zurich.
Received for publication March 24, 2023; accepted January 30, 2024.
The first two authors share first authorship.

DOI: 10.1097/PRS.0000000000011335

Nanofat is a mechanically emulsified fat for grafting that was first introduced in 2013.[1] Compared with microfat, which consists of intact adipocytes and microvessels, nanofat is a

Disclosure statements are at the end of this article, following the correspondence information.

Related digital media are available in the full-text version of the article on www.PRSJournal.com.

lipidic lysate produced through further emulsification and filtration steps that cause mechanical disruption of adipocytes and connective tissue. While microfat is primarily used to increase tissue volume, nanofat is suitable for intradermal application, which has opened the door to new therapeutic applications in regenerative medicine.[1–3] A growing body of literature has proven its effect on skin rejuvenation,[4–7] skin pigmentation,[8,9] hypertrophic and atrophic scar correction,[10–17] wound healing,[18–21] and cartilage repair.[22,23]

At the cellular and molecular levels, studies have described nanofat as being rich in adipose-derived stem cells, several different growth factors (vascular endothelial growth factor A, platelet-derived growth factor, and basic fibroblast growth factor), and functional microvessel segments.[1,24–27] Histopathologic evaluation of scars in patients after nanofat injection showed a significant increase in epidermal thickness, an increased number of collagen and elastic fibers, and neovascularization through increased expression of CD31.[16] However, the specific molecular components and pathways that drive tissue regeneration have only been analyzed superficially, because of the current lack of a standardized nanofat preparation method and the health and lifestyle variability among patient samples. Furthermore, while it is known that some cells and microvascular fragments remain viable after the mechanical emulsification process,[24,28] nanofat's main composition is high in lipidic and protein content. These characteristics make the molecular characterization of nanofat a challenge.

Using untargeted mass spectrometry, we recently detected 1702 proteins in matching microfat and nanofat samples from 18 healthy patients. Among them, 216 proteins were significantly enriched in nanofat, whereas only 130 proteins were enriched in microfat. Bioinformatic analysis of significantly enriched proteins in nanofat revealed their involvement in innate immunity responses (wound healing and coagulation), whereas enriched proteins in microfat were linked to cellular migration and extracellular matrix production. We found no significant difference between microfat and nanofat in growth factors or cytokines, which strongly suggests that the mechanical emulsification step does not affect the overall content of tissue regeneration biomarkers.[29] On the other hand, these observations hint of a further, as-yet unrecognized mechanism that might explain the clinically proven effect of nanofat.

Lipidomic profiling has gained attention over the past few years and become an emerging area of basic and translational research. Among 8 lipid classes, around 1.68 million lipid species can be identified, making their analysis a major challenge.[30] Once considered to be membrane components and energy storage reservoirs only, lipids are now recognized as important "mediators" in various biological processes, such as cell signaling, protein trafficking, growth, differentiation, and apoptosis.[31] A subset of lipid mediators, including sphingolipids and eicosanoids in particular, have been identified as key players during wound healing and tissue remodeling, thereby indicating a potential role in fat grafting.[32,33] With that, we aimed to investigate the lipid composition of microfat and nanofat samples.

PATIENTS AND METHODS

Patient Selection, Ethics, and Sample Collection

Microfat and nanofat samples were harvested from subcutaneous adipose tissue at the Department of Plastic Surgery and Hand Surgery, Zurich University Hospital. Fourteen male and female patients (age range, 21 to 81 years) with no comorbidities (eg, diabetes, obesity, or cancer) gave written consent with respect to the ethical guidelines of the local ethics committee (Business Administration System for Ethics Committees [BASEC] no. 2017-00261). Samples from smokers were excluded.

Nanofat was prepared as per Tonnard et al.[1] and as previously described.[29] Microfat samples served as nonmechanically processed controls. Samples were immediately mixed with a protease inhibitor cocktail (Merck, Darmstadt, Germany), snap-frozen in liquid nitrogen, and stored at −80°C until they were delivered to the Functional Genomics Center Zurich for sample processing and mass spectrometry (MS) analysis. The workflow from sample collection to data processing is shown in Figure 1.

Liquid Chromatography Tandem Mass Spectrometry Analysis

Polar Metabolites

Sample preparation for liquid chromatography (LC) tandem MS (LC-MS/MS) analyses was modified from the method used by Paglia et al.[34] A total of 50 µL of methanol extract was dried under nitrogen, reconstituted in 20 µL of water, and diluted with 80 µL of injection buffer (90% acetonitrile, 8.8% methanol, and 50 mM NH_4 acetate). After samples were vortexed and centrifuged (10,000 *g* at 4°C for 15 minutes), 50 µL of the supernatant was transferred into a glass vial (Total Recovery Vials; Waters, Milford, MA) for LC-MS/MS injection.

Metabolites were separated on an ultraperformance liquid chromatograph (nanoAcquity UPLC; Waters) equipped with a BEH amide capillary

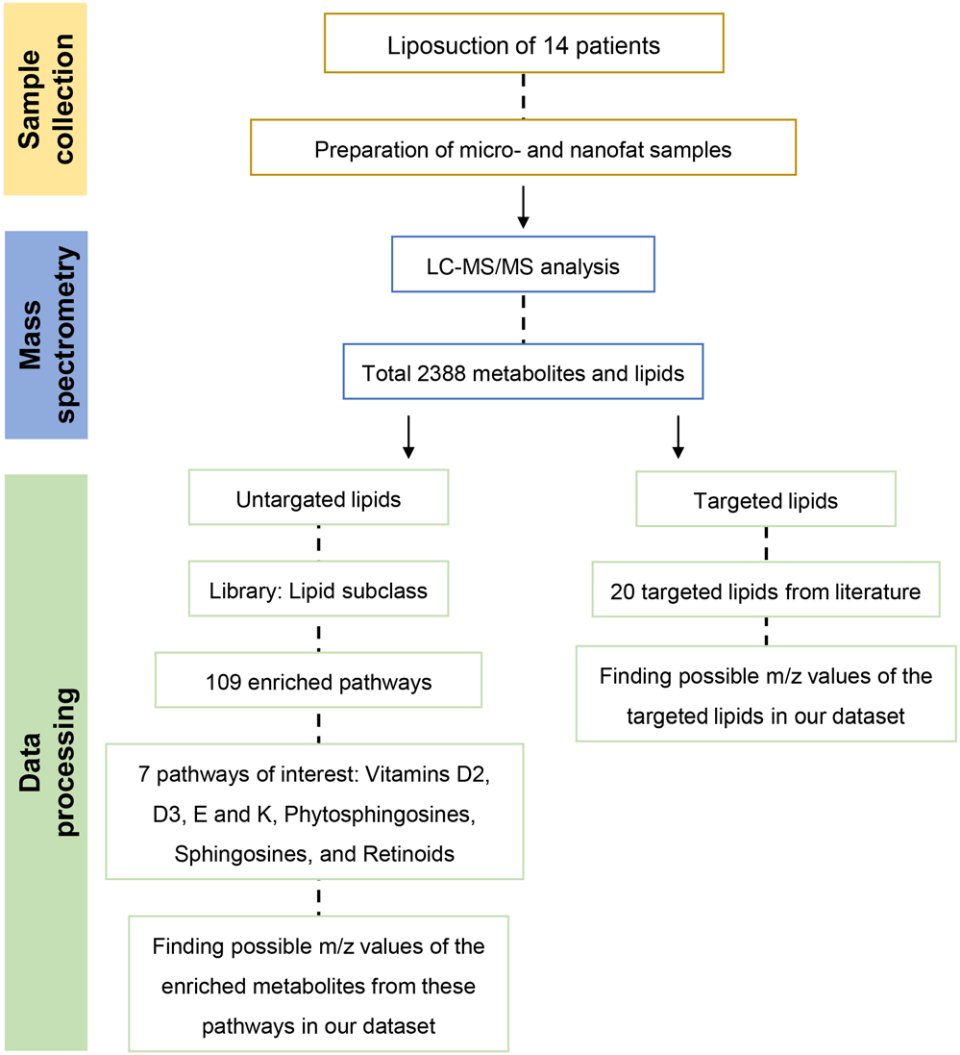

Fig. 1. Study flowchart. Fat harvesting was performed on 14 healthy patients who were screened for comorbidities. A total of 2388 metabolites and lipids were found in the samples using mass spectrometry. Metabolic pathway analysis within the lipid subclasses revealed 109 enriched pathways in microfat and nanofat. Some pathways of interest were analyzed further to define whether they were enriched in microfat or nanofat. In addition, 20 targeted lipids were selected for further analysis based on their possible roles in relevant mechanisms, such as wound healing, antiscarring effect, proliferation, tissue remodeling, hemostasis, and inflammation. Possible matches were then searched for according to the mass-to-charge ratio (*m/z*) values of these targeted lipids among the 2390 metabolites and lipids in the dataset. *LC-MS/MS*, liquid chromatography tandem mass spectrometry.

column (150 μm × 130 mm, 1.7-μm particle size; Waters). The solvent system consisted of buffer A (0.5 mM NH_4 acetate and 0.05% NH_4OH in water) and buffer B (0.5 mM NH_4 acetate and 0.05% NH_4OH in 95% acetonitrile). A gradient metabolite elution from 2% A to 50% A was applied for 10 minutes, with the flow rate reduced from 4 μL/min to 3 μL/min, followed by a washing step for 1 minute at 60% A, with a flow rate of 2.5 μL/min, and a re-equilibration for 5 minutes at 3 μL/min. The injection volume was 1 μL. The nanoAcquity UPLC was coupled to a Synapt G2-HDMS mass spectrometer (Waters) by a nano-ESI source. MS 1 and 2 data were acquired using negative polarization and an MSE over a mass range of 50 to 1200 mass-to-charge ratio (m/z) at a resolution greater than 20,000.[35]

Apolar Metabolites

A total of 100 μL of methanol extract was dried under nitrogen and reconstituted in 100 μL of

injection buffer (50% methanol). Samples were vortexed and centrifuged (10,000 *g* at 20°C for 15 minute). Fifty microliters of the supernatant was transferred to a glass vial (Waters) for LC-MS/MS injection. Lipids were separated in a nanoAcquity UPLC system (Waters) equipped with a High Strength Silica T3 capillary column (150 μm × 50 mm, 1.8-μm particle size; Waters). Samples were prepared in the same manner as used for the analysis of polar metabolites. Samples were then separated on the nanoAcquity UPLC using a solvent system consisting of buffer A (5 mM NH_4 acetate in 95% water and 5% acetonitrile) and buffer B (5 mM NH_4 acetate in 90% isopropanol and 10% acetonitrile).[36] A gradient metabolite elution from 95% A to 2% A was applied for 10 minutes, with the flow rate reduced from 3 μL/min to 2.5 μL/min, followed by a washing step for 5 minutes at 98% B, with a flow rate of 2.5 μL/min, and followed by 5 minutes of re-equilibration with a flow rate 3 μL/min. The injection volume was 1 μL. The injection volume was 1 μL. The nanoAcquity UPLC was coupled to a QExactive mass spectrometer (Thermo Fisher Scientific, Inc., Waltham, MA) by a nano–ESI source. MS data were acquired using positive and negative polarization and data-dependent acquisition (top 5). Full-scan MS spectra were acquired in profile mode from 80 to 1200 m/z, with an automatic gain control target of 1e6, an Orbitrap resolution of 70,000, and a maximum injection time of 200 msec. The five most intense charged (z = +1 or +2) precursor ions from each full scan were selected for collision-induced dissociation fragmentation. The precursor was accumulated with an isolation window of 0.4 Da, automatic gain control value of 5e4, a resolution of 17,500, and a 50-msec maximum injection time, and then fragmented with a normalized collision energy of 20 and 30 (arbitrary unit). Generated fragment ions were scanned in the linear trap. The minimal signal intensity for MS2 selection was set to 5e3.[37]

Statistical Analysis

Statistical analyses were conducted using IBM SPSS software and the MetaboAnalyst 5.0 web-based tool. The figures were prepared with GraphPad Prism 8 software (GraphPad Software, Inc., San Diego, CA). Normal distribution of the variables was determined by skewness and kurtosis ($P > 0.05$), and outliers were detected with the Tukey method. Targeted lipids were identified according to their mass-to-charge ratio, and a paired *t* test was conducted on the targeted lipids to detect differences in the intensity of the ions between microfat and nanofat. A metabolic pathway enrichment analysis based on a mummichog algorithm on untargeted lipids was run to determine the total number of significant hits per pathway. Briefly, MetaboAnalyst 5.0[38,39] determined the metabolic pathways from a list of metabolites (the user's uploaded set of mass-to-charge ratio features), considering all potential matches (isotopes/adducts).[40] These tentative compounds were then mapped onto known metabolic pathways for the selected organism (human). For each pathway, a hypergeometric *P* value was calculated.

RESULTS

Metabolic Pathway Analysis on Untargeted Lipids

Because it is challenging to correctly identify a particular peak based on its mass alone, we analyzed individual pathways rather than specific compounds. We uploaded a total of 2388 mass-to-charge ratio features for the metabolic pathway enrichment analysis, and found 109 significantly enriched pathways in microfat and nanofat. The visualization of the inspected enriched pathways, in accordance with the global Kyoto Encyclopedia of Genes and Genomes metabolic network, showed higher peak intensities of enriched pathways in microfat compared with nanofat. (**See Figure, Supplemental Digital Content 1**, which demonstrates enriched pathways in microfat and nanofat samples. The *blue-red* color scale represents peak intensities. The numbers on the right represent the mass-to-charge ratio values of possible pathways, ***http://links.lww.com/PRS/H99***. Created using the Metaboanalyst 5.0 software.) We also identified the total number of lipid metabolites found in our data within each pathway (hits total) and those that were significantly different between microfat and nanofat samples (hits sign). (**See Table, Supplemental Digital Content 2**, which illustrates the hits sign/hits total ratio above 0.1. A metabolic pathway analysis on untargeted lipids was performed to identify lipid subclasses in order of the hits significance/total, ***http://links.lww.com/PRS/H100***.) We continued our analysis by defining the significantly enriched lipids within pathways of interest detected by our metabolic pathway analysis. Our pathways of interest were vitamins D2, D3,[41] E, and K[42]; coumaric acids[43]; sphingosines[44]; phytosphingosines; and retinoids, due to their tissue-remodeling properties. The potential matches for the lipids within these pathways were determined with the metabolic pathway enrichment analysis using MetaboAnalyst 5.0 (Table 1).

Table 1. Significantly Enriched Metabolites within the Lipid Subclasses of Interest from the Metabolic Pathway Analysis

Lipid Subclass	Significantly Enriched Metabolites
Vitamin D2	1-a,24R,25-Trihydroxyvitamin D2
	(24R)-1α,24,25,26-Tetrahydroxyvitamin D2
Vitamin D3	Calcitriol
	Calcidiol
	Cholecalciferol
	Secalciferol
	1α,18-Dihydroxyvitamin D3/1α,18-dihydroxycholecalciferol
Vitamin E	β-Tocopherol
	δ-Tocopherol
Vitamin K	Vitamin K1 2,3-epoxide
Coumaric acids	2,5-Dimethoxycinnamic acid
	Phaseolic acid
Phytosphingosines	Dehydrophytosphingosine
Sphingosines	3-Ketosphingosine
Thromboxanes	Thromboxane B2
	11-Dehydro-2,3-dinor-TXB2; TXB1
Retinoids	Vitamin A

Differences between Microfat and Nanofat Samples in Selected Lipid Subclasses

Although metabolic pathway analysis identifies the differently enriched lipid mediators between microfat and nanofat, it does not differentiate which of the groups is significantly enriched in certain lipids. Therefore, we determined possible mass-to-charge ratio values for each enriched lipid (Table 1) according to the LIPID MAPS Structure Database, and found these values in our untargeted metabolomics data list. Two significantly enriched lipid mediators from the coumaric acid family, 2,5-dimethoxycinnamic acid (Fig. 2, *left*) ($t[13] = 4.021$, $P = 0.001$) and phaseolic acid (Fig 2, *right*) ($t[13] = 4.960$, $P < 0.001$), showed a higher intensity in nanofat samples in comparison to microfat.

Sphingosines and phytosphingosines had one significant compound hit each. Both 3-ketosphingosine (Fig. 3, *left*) ($t[13] = 5.596$, $P < 0.001$) and dehydrophytosphingosine (Fig. 3, *right*) ($t[13] = 4.341$, $P < 0.001$) were significantly higher in microfat.

Microfat samples also demonstrated an overall higher intensity in all lipids within retinoids (vitamin A: $t[13] = 7.343$, $P < 0.001$), vitamin D2 (1-α,24R,25-trihydroxyvitamin D2; $t[13] = 6.750$, $P < 0.001$; [24R]-1α,24,25,26-tetrahydroxyvitamin D2: $t[13] = 3.064$, $P = 0.009$), vitamin D3 (calcidiol: $t[13] = 3.132$, $P = 0.008$; secalciferol or calcitriol: $t[13] = 6.638$, $P < 0.001$; cholecalciferol: $t[13] = 5.545$, $P < 0.001$; 1α,18-dihydroxyvitamin D3: $t[13] = 6.750$, $P < 0.001$), vitamin E (δ-tocopherol: $t[13] = 6.406$, $P < 0.001$; β-tocopherol: $t[13] = 5.309$, $P < 0.001$), and vitamin K (vitamin K 1 2,3-epoxide: $t[13] = 8.096$, $P < 0.001$) (Fig. 4).

Exploration of Selected Lipid Mediators Linked to Tissue Regeneration Properties in Nanofat

The peak intensity of selected lipid mediators was compared between microfat and nanofat (Fig. 5). Among 6 lipid mediators that we identified (lysophosphatidic acid: $t[13] = 6.513$, $P < 0.001$;

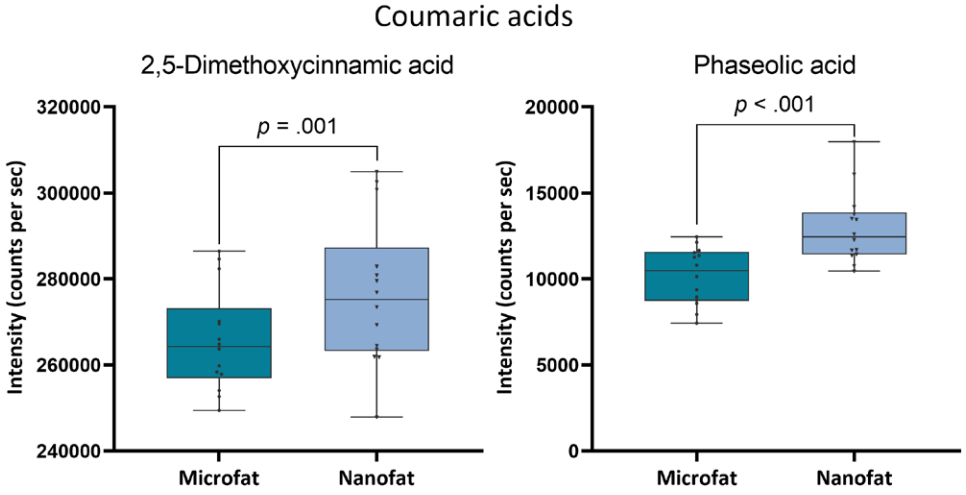

Fig. 2. MS peak intensities of coumaric acids in microfat and nanofat samples. Nanofat samples demonstrated a higher intensity in both (*left*) 2,5-dimethoxycinnamic acid and (*right*) phaseolic acid in comparison to microfat samples. All data are expressed as the mean ± SE, paired samples *t* test.

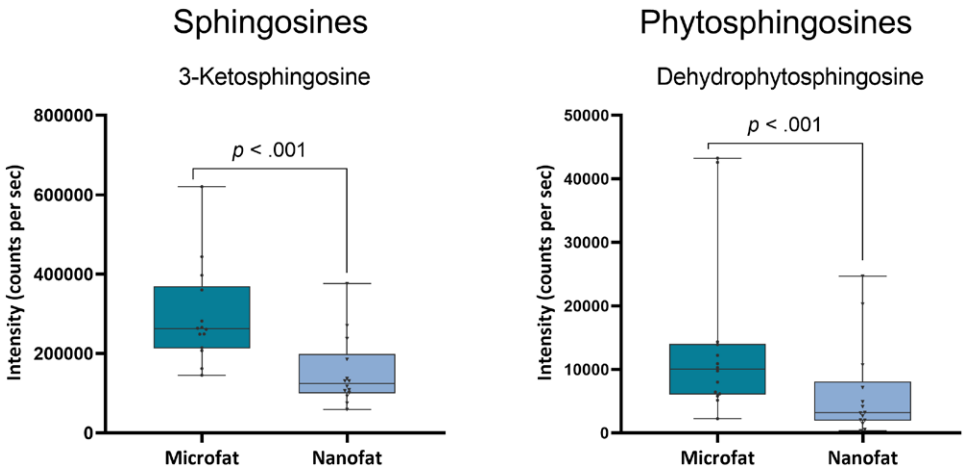

Fig. 3. MS peak intensities of sphingosines and phytosphingosines in microfat and nanofat samples. Both sphingosines and phytosphingosines had one significant compound hit each. In both compound hits, (*left*) 3-ketosphingosine and (*right*) dehyrophytosphingosine had a higher intensity in microfat samples than in nanofat samples. All data are expressed as the mean ± SE, paired samples *t* test.

docosahexanoic acid: $t[12] = 4.474$, $P < 0.001$; leukotriene [LT] B4: $t[11] = 1.363$, $P = 0.200$; prostaglandin [PG] E2: $t[13] = 2.541$, $P = 0.025$; and epoxyeicosatrienoic acid [EET]: $t[13] = 0.032$, $P = 0.965$), only PGI2 was higher in nanofat in comparison to microfat ($t[13] = 3.690$, $P = 0.003$).

DISCUSSION

To the best of our knowledge, this is the first study to analyze specific target lipids in autologous fat grafts. The lipidomic profiling of microfat and nanofat samples has allowed us to shed light on their lipidome in an effort to pinpoint differences between the two to better understand their unique clinical outcomes. The metabolic pathway enrichment analysis revealed 109 pathways with significant differences between microfat and nanofat samples. Our results show that the lipid profiles of microfat and nanofat samples differ significantly, possibly due to the mechanical fractionation of microfat to nanofat that disrupts adipocytes and connective tissue or to subsequent lipid release.

Past studies focused on the mechanism of action of autologous fat grafts and the influence of different processing techniques. In a secretome analysis of differently processed lipoaspirates, no differences in protein composition were found.[45] Although we recently detected a significantly different protein profile between microfat and nanofat samples, the use of different methods and, most importantly, different processing techniques precludes further comparison between the studies.[29] It has also been shown that mechanical processing does not affect the differentiation potential of adipose-derived stem cells; instead, only a decrease in adipocyte depots and an increase in the extracellular matrix occur based on histological examination.[46] Consequently, we presume there must be further unrecognized differences that elucidate the different regenerative capacities of microfat and nanofat samples.

Our research has allowed us to gain new and valuable insight into individual lipid mediators, specifically sphingolipids and eicosanoids, which are particularly imperative during wound healing and tissue remodeling.[32,33] Our analysis revealed significantly higher levels of coumaric acid in nanofat samples. Coumaric acids have been demonstrated to reduce oxidative stress and inflammatory reactions. Furthermore, the p-coumaric acid derivate exhibits antimelanogenic properties.[43,47,48] It is relevant to point out that p-coumaric acid cream has shown a skin lightening effect after application on fully tanned human skin. This could make the component of great interest as an active ingredient in skin lightening in hyperpigmentation/hypopigmentation or in improving the confluence of skin grafts,[48] and it serves as a possible explanation for the observed beneficial effects of nanofat on skin pigmentation.

We observed significantly higher peak intensities for the different fat-soluble vitamins in microfat, namely, vitamin D and its metabolites, vitamins E, K, and A. It was previously demonstrated that systemic administration of vitamin D improves human fat graft retention after autologous fat

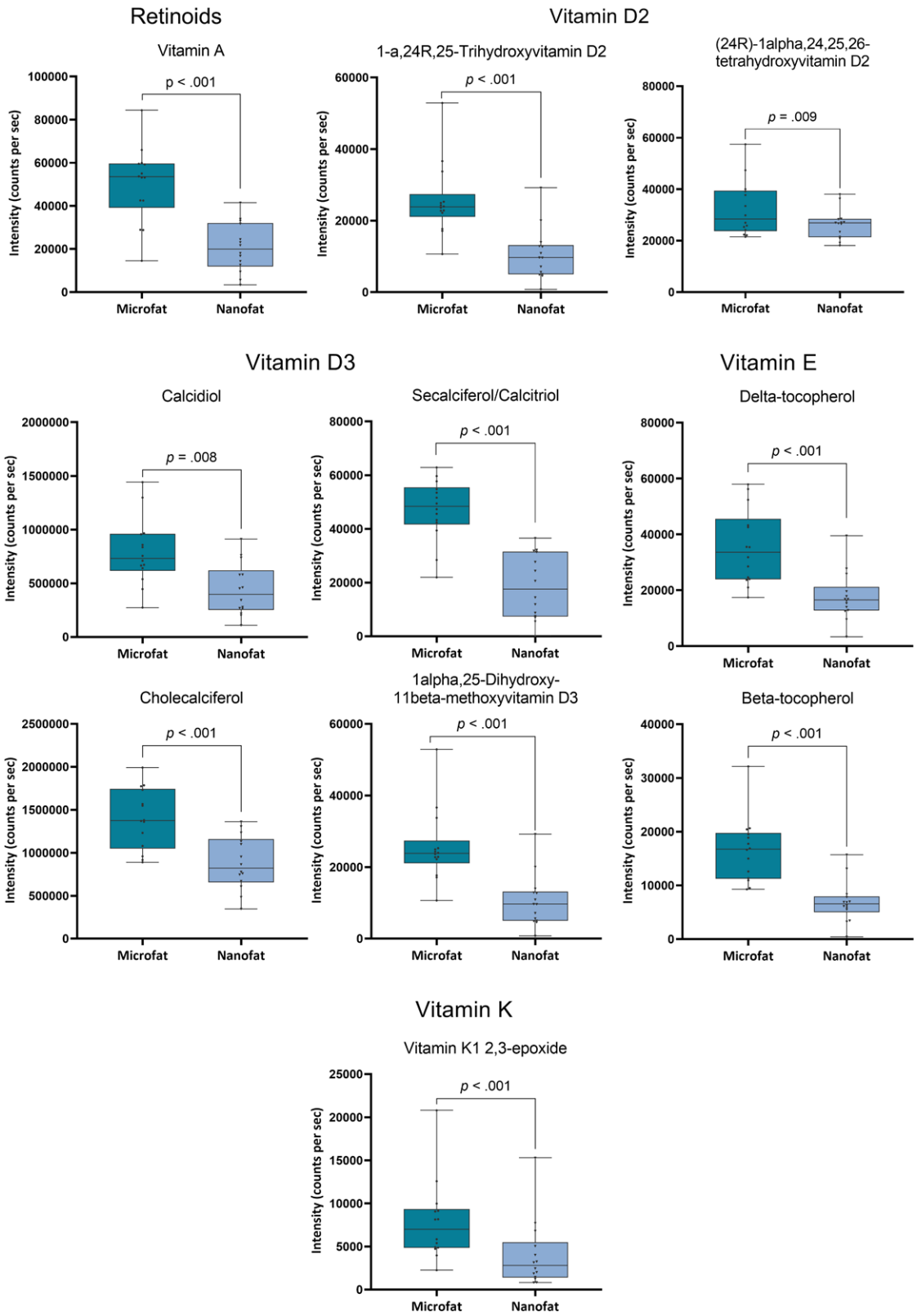

Fig. 4. MS peak intensities of vitamins in microfat and nanofat samples. Analyses detected significant compound hits in subclasses of (*above, left*) retinoids (vitamin A), (*above, right*) vitamin D2 (1-α,24R,25-trihydroxyvitamin D2, (24R)-1α,24,25,26-tetrahydroxyvitamin D2), (*center, left*) vitamin D3 (calcidiol, secalciferol or calcitriol, cholecalciferol, 1α,18-dihydroxyvitamin D3), (*center, right*) vitamin E (δ- and β-tocopherol), and (*below*) vitamin K (vitamin K1 2,3-epoxide). Microfat samples demonstrated higher intensity in all significant compound hits of these subclasses. All data are expressed as mean ± SE, paired samples *t* test.

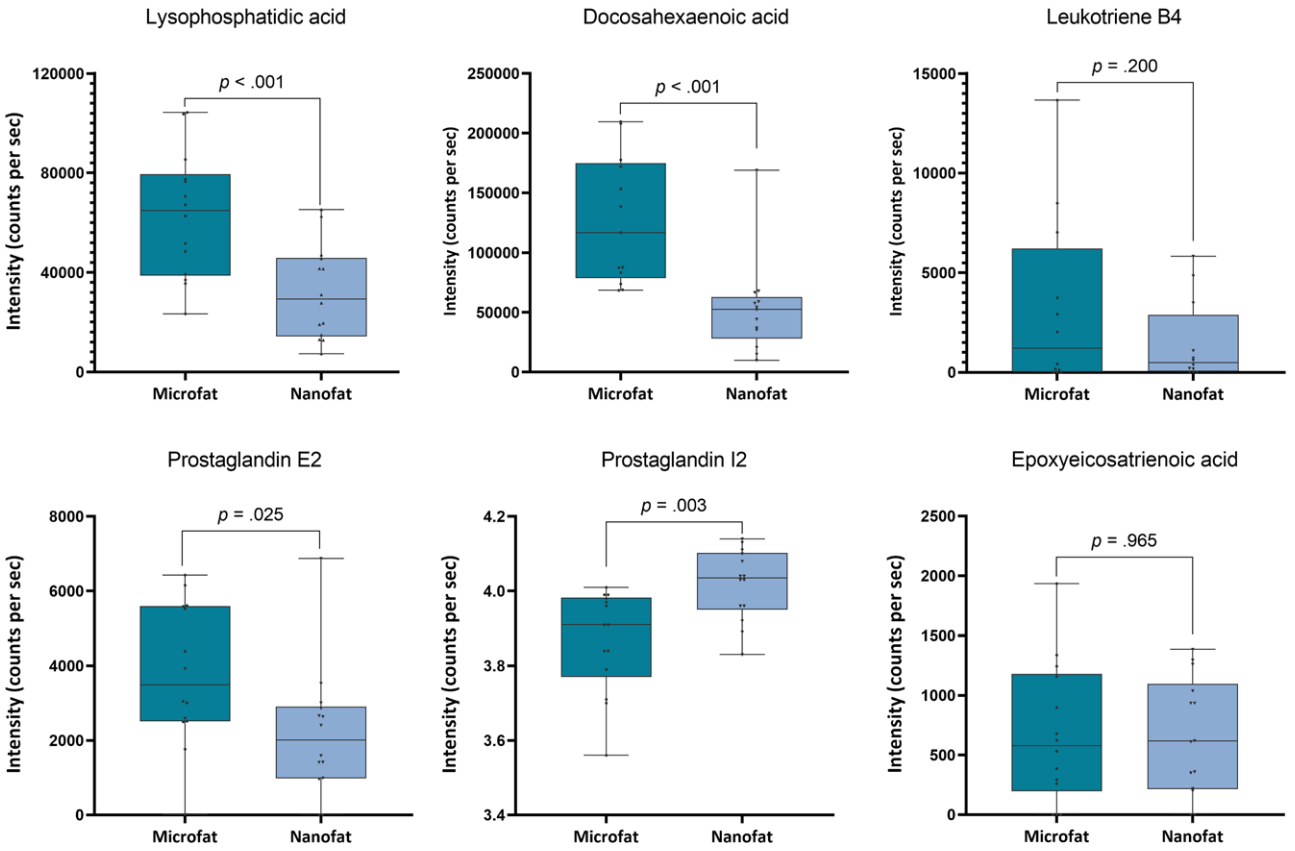

Fig. 5. MS peak intensities of targeted lipids that have a role in wound healing. Microfat samples demonstrated a higher intensity in (*above, left*) lysophosphatic acid and (*above, center*) docosahexaenoic acid. The peak intensity of (*above, right*) LTB4 did not differ between nanofat and microfat samples. While microfat samples showed higher intensity in (*below, left*) PGE2, they showed lower intensity than nanofat samples in (*below, center*) PGI2. There was no difference detected between microfat and nanofat samples in the intensity of (*below, right*) EET. All data are expressed as mean ± SE, paired samples *t* test.

grafting in a mouse xenograft model, suggesting a critical role in fat-grafting procedures.[49] In contrast to nanofat, microfat is specifically applied for volume augmentation because of its intact adipocytes. Considering this, it is interesting that vitamin D appears to be present in higher levels in microfat, which might suggest that it could possibly support the integration of adipocytes in the context of volume augmentation. Several studies have also reported that treatment with one of the aforementioned vitamins improves scar quality and promotes wound healing.[50–53]

MS also revealed differences in eicosanoids, with significantly higher amounts of prostacyclin (PGI2) in nanofat samples. Eicosanoids are derived from membrane fatty acids and include a number of different lipid mediators, such as PGs, LTs, and so-called specialized proresolving mediators.[32] PGI2 is known to act as a vasodilator that maintains adequate blood flow to peripheral tissue. In the specific context of nanofat grafting, we hypothesize that PGI2 might be responsible for promoting vascularization and thus the distribution and action of growth factors and cytokines in the surrounding tissue. Various studies have also highlighted the importance of PGI2 in preventing fibrosis and fibrotic progression,[54] which could serve as a conceivable explanation for the beneficial effect of nanofat on scar and tissue quality.

In contrast, there were significantly higher amounts of its counterpart, PGE2, in microfat samples. Besides promoting angiogenesis and fibroblast and keratinocyte proliferation, PGE2 plays an important role in macrophage polarization.[55] In the late phase of wound healing, the transition of the proinflammatory M1 phenotype macrophage to the M2 regenerating phenotype is necessary to promote normal wound healing. PGE2 was found to enhance wound closure by promoting the conversion of the M2 phenotype of macrophages.[32,56] In chronic wounds, this transformation is impaired, and the M1 phenotype is predominant.[32,56] Recent studies have mentioned that treatment with autologous fat grafting improved

the healing of acute burns and infected ulcers.[19–21] Considering the limitations of this study and the complexity of wound-healing mechanisms at the cellular and protein levels, it is possible that PGE2 is one of many components contributing to the wound-healing properties of fat grafting. The current literature lacks a comparison of the wound-healing effectiveness of microfat and nanofat.[57] Therefore, we hypothesize that the higher PGE2 levels detected in microfat could be one component promoting wound healing.

The peak intensities of LTB4 and EET, which also belong to the group of eicosanoids, did not differ between microfat and nanofat samples. In contrast to PGs, LT is known to be associated with impaired wound healing. As such, LT receptor antagonists were found to enhance wound closure by modulating the inflammatory response.[58,59] EET acts as a vasodilator and is known for its pro-angiogenic but antiinflammatory potential. In one study, topical application of EET on mouse ear wounds improved ischemic wound healing, which was attributed to a significant increase in the expression of stromal cell–derived factor, vascular endothelial growth factor, and transforming growth factor-β1.[60] Hence, EET has been proposed as a potential therapeutic agent for various pathologies of wound healing. Synthetic production of EET is time-consuming and expensive. Therefore, autologous fat grafting could be an accessible source of EET for the treatment of wounds. A similar acceleration of wound healing has also been reported for treatment with docosahexaenoic acid[61] and lysophosphatidic acid,[62] both of which were found in higher concentrations in microfat.

Limitations

Our study has several limitations with regard to the data analysis and study protocol. Currently, we can only discuss and interpret our results from a theoretical point of view. A further analysis of patient-specific differences was outside the exploratory scope of this study. Although none of the patients had comorbidities, it is well-known that the lipidome is significantly influenced by many factors, such as lifestyle, sex, age, and diet, that could affect the lipid composition of the autologous fat graft and, therefore, influence its therapeutic efficacy and the surgical outcome.[63] Furthermore, fat samples were harvested from body regions that can also differ in their lipid composition.[64] Our future research will focus on patient-specific differences in lipid composition of autologous fat grafts in relation to postoperative outcomes, such as the degree of scar remodeling after fat grafting.

CONCLUSIONS

We would like to report this as the first study to analyze the lipidomic profile of autologous fat samples and to provide evidence that the mechanical fractionation of microfat to nanofat significantly alters lipid composition. Using 109 enriched pathways, higher levels of fat-soluble vitamins were found in microfat, whereas anti-inflammatory, antifibrotic and antimelanogenic lipid mediators were particularly elevated in nanofat samples. This study contributes to understanding the composition of nanofat and microfat at a molecular level. Further investigation of their therapeutic effects is warranted.

Nicole Lindenblatt, MD
Department of Plastic Surgery and Hand Surgery
University Hospital Zurich
Raemistrasse 100
8091 Zurich, Switzerland
nicole.lindenblatt@usz.ch
@nic.lindenblatt

DISCLOSURE

Dr. Lindenblatt acts as a scientific advisor and symposium speaker for Medical Microinstruments. The other authors have no financial interests to declare.

ACKNOWLEDGMENTS

The authors are grateful to Dr. Endre Laczko of the Functional Genomics Center Zurich for performing mass spectrometry and raw data processing and for providing helpful insight in data interpretation. This study was part of the SKINTEGRITY.CH research consortium, and was partly funded by it. The study was funded by research grants from the Novartis Foundation, Switzerland, and the Foundation for Scientific Research of the University of Zurich, Switzerland.

REFERENCES

1. Tonnard P, Verpaele A, Peeters G, Hamdi M, Cornelissen M, Declercq H. Nanofat grafting: basic research and clinical applications. *Plast Reconstr Surg.* 2013;132:1017–1026.
2. Lindenblatt N, van Hulle A, Verpaele AM, Tonnard PL. The role of microfat grafting in facial contouring. *Aesthet Surg J.* 2015;35:763–771.
3. Rihani J. Microfat and nanofat: when and where these treatments work. *Facial Plast Surg Clin North Am.* 2019;27:321–330.
4. Liang ZJ, Lu X, Li DQ, et al. Precise intradermal injection of nanofat-derived stromal cells combined with platelet-rich fibrin improves the efficacy of facial skin rejuvenation. *Cell Physiol Biochem.* 2018;47:316–329.
5. Menkes S, Luca M, Soldati G, Polla L. Subcutaneous injections of nanofat adipose-derived stem cell grafting in facial rejuvenation. *Plast Reconstr Surg Glob Open* 2020;8:e2550.
6. Mesguich Batel F, Bertrand B, Magalon J, et al. [Treatment of wrinkles of the upper lip by emulsified fat or

"nanofat": biological and clinical study about 4 cases]. *Ann Chir Plast Esthet.* 2018;63:31–40.
7. Tonnard P, Verpaele A, Carvas M. Fat grafting for facial rejuvenation with nanofat grafts. *Clin Plast Surg.* 2020;47:53–62.
8. Ziade G, Karam D. Emulsified fat and nanofat for the treatment of dark circles. *Dermatol Ther.* 2020;33:e14100.
9. Bhooshan LS, Devi MG, Aniraj R, Binod P, Lekshmi M. Autologous emulsified fat injection for rejuvenation of scars: a prospective observational study. *Indian J Plast Surg.* 2018;51:77–83.
10. Gu Z, Li Y, Li H. Use of condensed nanofat combined with fat grafts to treat atrophic scars. *JAMA Facial Plast Surg.* 2018;20:128–135.
11. Uyulmaz S, Sanchez Macedo N, Rezaeian F, Giovanoli P, Lindenblatt N. Nanofat grafting for scar treatment and skin quality improvement. *Aesthet Surg J.* 2018;38:421–428.
12. Tenna S, Cogliandro A, Barone M, et al. Comparative study using autologous fat grafts plus platelet-rich plasma with or without fractional CO2 laser resurfacing in treatment of acne scars: analysis of outcomes and satisfaction with FACE-Q. *Aesthetic Plast Surg.* 2017;41:661–666.
13. Kemaloglu CA, Ozyazgan I, Gonen ZB. Immediate fat and nanofat-enriched fat grafting in breast reduction for scar management. *J Plast Surg Hand Surg.* 2020;55:173–180.
14. Behrangi E, Moradi S, Ghassemi M, et al. The investigation of the efficacy and safety of stromal vascular fraction in the treatment of nanofat-treated acne scar: a randomized blinded controlled clinical trial. *Stem Cell Res Ther.* 2022;13:298.
15. Pons S, Jammet P, Galmiche S, et al. Nanofat and platelet-rich plasma injections used in a case of severe acne scars. *J Stomatol Oral Maxillofac Surg.* 2022;123:572–575.
16. Rageh MA, El-Khalawany M, Ibrahim SMA. Autologous nanofat injection in treatment of scars: a clinico-histopathological study. *J Cosmet Dermatol.* 2021;20:3198–3204.
17. Jan SN, Bashir MM, Khan FA, et al. Unfiltered Nanofat Injections Rejuvenate Postburn Scars of Face. *Ann Plast Surg.* 2019;82:28–33.
18. Kemaloglu CA. Nanofat grafting under a split-thickness skin graft for problematic wound management. *Springerplus* 2016;5:138.
19. Segreto F, Marangi GF, Nobile C, et al. Use of platelet-rich plasma and modified nanofat grafting in infected ulcers: technical refinements to improve regenerative and antimicrobial potential. *Arch Plast Surg.* 2020;47:217–222.
20. Abouzaid AM, El Mokadem ME, Aboubakr AK, Kassem MA, Al Shora AK, Solaiman A. Effect of autologous fat transfer in acute burn wound management: a randomized controlled study. *Burns* 2022;48:1368–1385.
21. Rohani Ivari J, Mahdipour E. Adipose tissue versus stem cell-derived small extracellular vesicles to enhance the healing of acute burns. *Regen Med.* 2021;16:629–641.
22. Chen Z, Ge Y, Zhou L, et al. Pain relief and cartilage repair by nanofat against osteoarthritis: preclinical and clinical evidence. *Stem Cell Res Ther.* 2021;12:477.
23. Han Z, Bai L, Zhou J, et al. Nanofat functionalized injectable super-lubricating microfluidic microspheres for treatment of osteoarthritis. *Biomaterials* 2022;285:121545.
24. Weinzierl A, Harder Y, Schmauss D, Menger MD, Laschke MW. Boosting tissue vascularization: nanofat as a potential source of functional microvessel segments. *Front Bioeng Biotechnol.* 2022;10:820835.
25. Pallua N, Grasys J, Kim BS. Enhancement of progenitor cells by two-step centrifugation of emulsified lipoaspirates. *Plast Reconstr Surg.* 2018;142:99–109.
26. Wei H, Gu SX, Liang YD, et al. Nanofat-derived stem cells with platelet-rich fibrin improve facial contour remodeling and skin rejuvenation after autologous structural fat transplantation. *Oncotarget* 2017;8:68542–68556.
27. Lo Furno D, Tamburino S, Mannino G, et al. Nanofat 2.0: experimental evidence for a fat grafting rich in mesenchymal stem cells. *Physiol Res.* 2017;66:663–671.
28. Tonnard P, Verpaele A, Peeters G, Hamdi M, Cornelissen M, Declercq H. Nanofat grafting: basic research and clinical applications. *Plast Reconstr Surg.* 2013;132:1017–1026.
29. Sanchez-Macedo N, McLuckie M, Grunherz L, Lindenblatt N. Protein profiling of mechanically processed lipoaspirates: discovering wound healing and antifibrotic biomarkers in nanofat. *Plast Reconstr Surg.* 2022;150:341e–354e.
30. Li L, Han J, Wang Z, et al. Mass spectrometry methodology in lipid analysis. *Int J Mol Sci* . 2014;15:10492–10507.
31. Aldana J, Romero-Otero A, Cala MP. Exploring the lipidome: current lipid extraction techniques for mass spectrometry analysis. *Metabolites* 2020;10:231.
32. Yasukawa K, Okuno T, Yokomizo T. Eicosanoids in skin wound healing. *Int J Mol Sci* . 2020;21:8435.
33. Aoki M, Aoki H, Mukhopadhyay P, et al. Sphingosine-1-phosphate facilitates skin wound healing by increasing angiogenesis and inflammatory cell recruitment with less scar formation. *Int J Mol Sci* . 2019;20:3381.
34. Paglia G, Williams JP, Menikarachchi L, et al. Ion mobility derived collision cross sections to support metabolomics applications. *Anal Chem.* 2014;86:3985–3993.
35. Koch LM, Birkeland ES, Battaglioni S, et al. Cytosolic pH regulates proliferation and tumour growth by promoting expression of cyclin D1. *Nat Metab.* 2020;2:1212–1222.
36. Schlatholter I, Broggini GAL, Streb S, Studer B, Patocchi A. Field study of the fire-blight-resistant cisgenic apple line C44.4.146. *Plant J.* 2023;113:1160–1175.
37. Drozdzyk K, Sawicka M, Bahamonde-Santos MI, et al. Cryo-EM structures and functional properties of CALHM channels of the human placenta. *Elife* 2020;9:e55853.
38. Xia J, Psychogios N, Young N, Wishart DS. MetaboAnalyst: a web server for metabolomic data analysis and interpretation. *Nucleic Acids Res.* 2009;37(Web Server issue):W652–W660.
39. Metaboanalyst. Available at: https://www.metaboanalyst.ca/. Accessed February 2, 2023.
40. Pang Z, Zhou G, Ewald J, et al. Using MetaboAnalyst 5.0 for LC-HRMS spectra processing, multi-omics integration and covariate adjustment of global metabolomics data. *Nat Protoc.* 2022;17:1735–1761.
41. Crescioli C. Vitamin D restores skeletal muscle cell remodeling and myogenic program: potential impact on human health. *Int J Mol Sci.* 2021;22:1760.
42. Tang S, Ruan Z, Ma A, Wang D, Kou J. Effect of vitamin K on wound healing: a systematic review and meta-analysis based on preclinical studies. *Front Pharmacol.* 2022;13:1063349.
43. Boo YC. p-Coumaric acid as an active ingredient in cosmetics: a review focusing on its antimelanogenic effects. *Antioxidants (Basel)* 2019;8:379.
44. Ogle ME, Sefcik LS, Awojoodu AO, et al. Engineering in vivo gradients of sphingosine-1-phosphate receptor ligands for localized microvascular remodeling and inflammatory cell positioning. *Acta Biomater.* 2014;10:4704–4714.
45. Prantl L, Eigenberger A, Klein S, et al. Shear force processing of lipoaspirates for stem cell enrichment does not affect secretome of human cells detected by mass spectrometry in vitro. *Plast Reconstr Surg.* 2020;146:749e–758e.
46. Eigenberger A, Felthaus O, Schratzenstaller T, Haerteis S, Utpatel K, Prantl L. The effects of shear force-based processing of lipoaspirates on white adipose tissue and the

differentiation potential of adipose derived stem cells. *Cells* 2022;11:2543.
47. An SM, Koh JS, Boo YC. p-Coumaric acid not only inhibits human tyrosinase activity in vitro but also melanogenesis in cells exposed to UVB. *Phytother Res.* 2010;24:1175–1180.
48. Seo YK, Kim SJ, Boo YC, Baek JH, Lee SH, Koh JS. Effects of p-coumaric acid on erythema and pigmentation of human skin exposed to ultraviolet radiation. *Clin Exp Dermatol.* 2011;36:260–266.
49. Leftwich PA, Lee PL, Loder S, et al. Vitamin D improves autologous fat graft retention. *Plast Reconstr Surg Glob Open* 2021;9(7 Suppl):40–41.
50. Tanaydin V, Conings J, Malyar M, van der Hulst R, van der Lei B. The role of topical vitamin E in scar management: a systematic review. *Aesthet Surg J.* 2016;36:959–965.
51. Akoh CC, Orlow SJ. A review of vitamin D and scarring: the potential for new therapeutics. *J Drugs Dermatol.* 2020;19:742–745.
52. Pazyar N, Houshmand G, Yaghoobi R, Hemmati AA, Zeineli Z, Ghorbanzadeh B. Wound healing effects of topical vitamin K: a randomized controlled trial. *Indian J Pharmacol.* 2019;51:88–92.
53. Polcz ME, Barbul A. The role of vitamin A in wound healing. *Nutr Clin Pract.* 2019;34:695–700.
54. Li K, Zhao J, Wang M, et al. The roles of various prostaglandins in fibrosis: a review. *Biomolecules* 2021;11:789.
55. Pils V, Terlecki-Zaniewicz L, Schosserer M, Grillari J, Lammermann I. The role of lipid-based signalling in wound healing and senescence. *Mech Ageing Dev.* 2021;198:111527.
56. Zhang S, Liu Y, Zhang X, et al. Prostaglandin E2 hydrogel improves cutaneous wound healing via M2 macrophages polarization. *Theranostics* 2018;8:5348–5361.
57. Malik D, Luck J, Smith OJ, Mosahebi A. A systematic review of autologous fat grafting in the treatment of acute and chronic cutaneous wounds. *Plast Reconstr Surg Glob Open* 2020;8:e2835.
58. Guimaraes FR, Sales-Campos H, Nardini V, et al. The inhibition of 5-lipoxygenase (5-LO) products leukotriene B4 (LTB4) and cysteinyl leukotrienes (cysLTs) modulates the inflammatory response and improves cutaneous wound healing. *Clin Immunol.* 2018;190:74–83.
59. Ramalho T, Filgueiras L, Silva-Jr IA, Pessoa AFM, Jancar S. Impaired wound healing in type 1 diabetes is dependent on 5-lipoxygenase products. *Sci Rep.* 2018;8:14164.
60. Sander AL, Jakob H, Sommer K, et al. Cytochrome P450-derived epoxyeicosatrienoic acids accelerate wound epithelialization and neovascularization in the hairless mouse ear wound model. *Langenbecks Arch Surg.* 2011;396:1245–1253.
61. Aytac A, Demir CI, Alagoz MS. Docosahexaenoic acid improves diabetic wound healing in a rat model by restoring impaired plasticity of macrophage progenitor cells. *Plast Reconstr Surg.* 2021;148:848e–849e.
62. Lei L, Su J, Chen J, Chen W, Chen X, Peng C. The role of lysophosphatidic acid in the physiology and pathology of the skin. *Life Sci.* 2019;220:194–200.
63. Mir SA, Chen L, Burugupalli S, et al. Population-based plasma lipidomics reveals developmental changes in metabolism and signatures of obesity risk: a mother-offspring cohort study. *BMC Med.* 2022;20:242.
64. Al-Sari N, Suvitaival T, Mattila I, et al. Lipidomics of human adipose tissue reveals diversity between body areas. *PLoS One* 2020;15:e0228521.